Environmental Challenges 7 (2022) 100446

Contents lists available at ScienceDirect

Environmental Challenges

journal homepage: www.elsevier.com/locate/envc

# Rainfall and temperature changes under different climate scenarios at the watersheds surrounding the Ngorongoro Conservation Area in Tanzania

Mohamed Mwabumba[a,*], Brijesh K. Yadav[b], Mwemezi J. Rwiza[a], Isaac Larbi[c], Sam-Quarcoo Dotse[c], Andrew Manoba Limantol[c], Solomon Sarpong[d], Daniel Kwawuvi[e]

[a] The Nelson Mandela African Institution of Science and Technology, PO Box 447, Arusha, Tanzania
[b] Indian Institute of Technology (IIT.) Roorkee, Uttarakhand, 247667, India
[c] School of Sustainable Development, University of Environment and Sustainable Development, Somanya, Ghana
[d] School of Natural and Environmental Sciences, University of Environment and Sustainable Development, Somanya, Ghana
[e] Climate Change and Water Resources, West African Science Service Centre on Climate Change and Adapted Land Use (WASCAL), Université d'Abomey-Calavi, Cotonou, Benin

ARTICLE INFO

*Keywords:*
Rainfall
Temperature
Projection
SDSM
Regional climate models
Ngorongoro conservation area

ABSTRACT

Considering the high vulnerability of Northern Tanzania to climate change, an in-depth assessment at the local scale is required urgently to formulate sustainable adaptations measures. Therefore, this study analyzed the future (2021-2050) changes in rainfall and temperature under the representative concentration pathways (RCP4.5 and RCP8.5) for the watersheds surrounding the Ngorongoro Conservation Area (NCA) at a spatio-temporal scale relative to the observed historical (1982-2011) period. The climate change analysis was performed at monthly and annual scale using outputs from a multi-model ensemble of Regional Climate Models (RCMs) and statistically downscaled Global Climate Models (GCMs). The performance of the RCMs were evaluated, and the downscaling of the GCMs were performed using Statistical Downscaling System Model (SDSM) and LARS-WG, with all the models indicating a higher accuracy at monthly scale when evaluated using statistical indicators such as correlation (*r*), Nash-Sutcliff Efficiency (NSE) and percentage bias (PBIAS). The results show an increase in the mean annual rainfall and temperature in both RCPs. The percentage change in rainfall indicated an increase relative to historical data for all seasons under both RCPs, except for the June, July, August and September (JJAS) season, which showed a decrease in rainfall. Spatially, rainfall would increase over the entire basin under both RCPs with higher increase under RCP4.5. Similar spatial increase results are also projected for temperature under both RCPs. The results of this study provide vital information for the planning and management of the studied watershed under changing climatic conditions.

## 1. Introduction

Climate change has become a global threat that significantly affects the water sector (Adhikari et al., 2015, Amirabadizadeh et al., 2016). Africa is expected to be seriously affected by the impacts of climate change due to the high dependency of economy on natural resources in the region (Adhikari et al., 2015). The region's water resources are already affected by the rapid population growth, urbanization, intensive agriculture, and hydropower demand. Therefore, climatic change poses significant challenges to the sustainability of water resources, especially in developing countries (Adhikari et al., 2015, Amirabadizadeh et al., 2016, Huang et al., 2011). It is one of the major drivers for environmental changes, leading to socio-economic implications related to the hydrological processes. With increasing temperatures and fluctuating precipitation, it is expected that water availability will decrease significantly in the future (Huang et al., 2011, Bessah et al., 2021). For sustainability, water resources need proper planning and management, taking into consideration the site-prevailing climate change assessment (Bessah et al., 2019).

To assess the consequences of climate change on different sectors, global impact assessment studies have been carried out using the General Circulation Models (GCMs). The GCMs have been widely used to assess the future climate based on energy and mass balance equations (Adhikari et al., 2015, Chiew et al., 2009) and their ability to capture the physical processes occurring in the climate system, which include the atmosphere, ocean, and land (Cooper et al., 2008). However, due to the coarse resolution of the available GCMs, local features such as topography and the convective clouds cannot be resolved

* Corresponding author.
*E-mail addresses:* mwabumbam@nm-aist.ac.tz (M. Mwabumba), brijesh.yadav@hy.iitr.ac (B.K. Yadav), mwemezi.rwiza@nm-aist.ac.tz (M.J. Rwiza), ilarbi@uesd.edu (I. Larbi), sqdotse@uesd.edu.gh (S.-Q. Dotse), amlimantol@uesd.edu.gh (A.M. Limantol), ssarpong@uesd.edu (S. Sarpong), danielkwawuvi@gmail.com (D. Kwawuvi).

https://doi.org/10.1016/j.envc.2022.100446
Received 30 August 2021; Received in revised form 23 December 2021; Accepted 9 January 2022

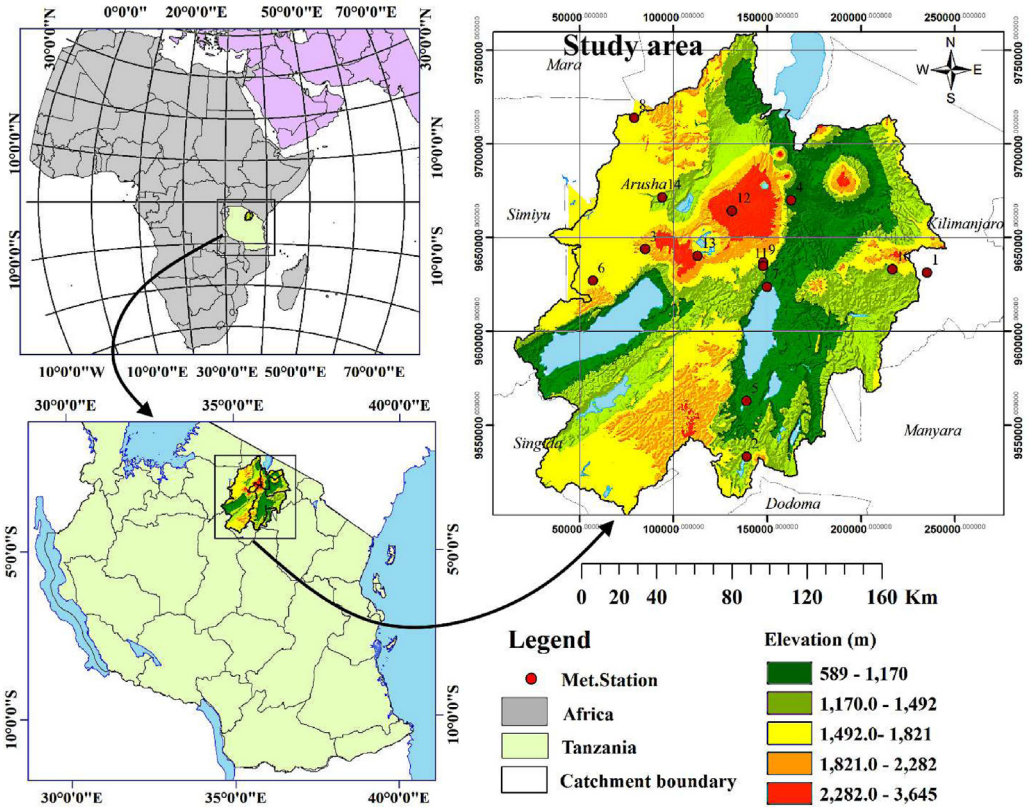


**Fig. 1.** Map of Africa (top left) indicating Tanzania (bottom left) and the Ngorongoro Conservation Area (NCA), and surroundings within 50km grid (right). The red dots on the NCA are the individual meteorological stations.

(Donat et al., 2016). Consequently, GCMs are not suitable for local-scale hydrological studies in response to climate change (Amirabadizadeh et al., 2016, Donat et al., 2016). To make use of the GCM for the hydrological impact studies, downscaling techniques are usually applied. There are two downscaling methods: 1) Dynamical and 2) Statistical. These methods are used for addressing the challenge of the GCM spatial resolution. This is achieved by connecting the large-scale atmospheric climate variables with the local-scale climate parameters. These downscaling methods convert the coarse-resolution GCM output into a finer resolution for a target geographical area (Saraf and Regulwar, 2016, Hashmi et al., 2009, Gebrechorkos et al., 2019).

The dynamical method uses the GCM output as the boundary condition to produce regional/local information at a resolution ranging from 5 to 50 km. This method provides information on the influence of orographic features on climatic variables (Gebrechorkos et al., 2019, Wilby and Dawson, 2013). On the other hand, statistical downscaling applies the empirical relationship between local observations (predictands) and the GCMs' predictor variables. Using statistical downscaling is computationally easy and transferable. The Statistical Downscaling System Model (SDSM) is one of the most applied climate downscaling models for regional and local climate impact studies. The SDSM is an open-access software developed using a stochastic weather generator and transferred statistical function method. The model has been used in several studies across East Africa at the regional and local scales using the GCM outputs (Estes et al., 2006). The usefulness of the SDSM is linked to its ability to capture interannual climate variability (Hashmi et al., 2009, Gebrechorkos et al., 2019). Furthermore, in the absence of the ground-based data, high-resolution satellite-based products and reanalysis products may be used to generate high-resolution station-based rainfall and temperature weather series (Saraf and Regulwar, 2016, Gebrechorkos et al., 2018).

Despite the significant progress in climate change impact assessment studies, a comprehensive basin-scale study attributable to national level water availability is necessary for Tanzania. Also, little is known about climate change impacts on hydrology and water resources in Tanzania, particularly at the watershed level. Moreover, there are limited studies carried out using statistical downscaling to assess the impacts of climate change at a local scale (Gebrechorkos et al., 2019, Gulacha and Mulungu, 2017). As hydrological possesses are site-specific, studies at the watershed level are needed to better manage the little available water resources.

The Ngorongoro Conservation Area (NCA) is one of the major hotspots of tourism and biodiversity on the African continent. The NCA is also an essential ecosystem for migrating wild ungulates from the Serengeti National Park during the dry season (Estes et al., 2006, Mkiramweni et al., 2016). The area is at high risk of climate change impacts due to the increased frequency of drought conditions and limited availability of water resources for people and wildlife (Tarver et al., 2019). Considering the high vulnerability of this area to climate change, an in-depth local-scale climatic assessment is required. Therefore, the focus of the present study was to analyze the future changes in the local climate under RCP4.5 and RCP8.5 climate scenarios at the watersheds surrounding the NCA using ensemble mean of CORDEX-Africa RCMs data and statistically downscaled rainfall and temperature outputs using SDSM and LARS-WG statistical downscaling tools.

## 2. Materials and Methods

### 2.1. Study area

The NCA is located in the northern part of Tanzania between latitudes 2.5° and 3.6° S and between longitudes 34.0° and 36.0° E with an area coverage of 8,283 km$^2$. The area is surrounded by watersheds covering an area of about 33,452 km$^2$ from latitude 2.2° to 4.5° S and longitude 34.0° to 36.7° E (Fig. 1). The NCA is characterized by moist and misty conditions, where temperatures in the semi-arid zone can fall

as low as 2°C in June/July, and often rises to 35°C in February (Masao et al., 2015). Rainfall in this area is seasonal and highly variable, ranging from 400 to 600 mm/year over the arid lowland plains in the west and from 1000 to1200 mm/year over the highland forested areas in the east (Lawuo et al., 2014). The NCA is characterized by a bimodal seasonal variability with two wet and two dry seasons. The wet periods are observed from October to December and March to May. A short dry season expands from January to February and a long dry period between June and September (Żaba and Gaidzik, 2011a).

The NCA is a highly diverse ecosystem and is broadly categorized into five different zones: the Crater Highlands, the Salei Plains, the Gol Mountains, the Serengeti Plains, and the Kakesio Mountain (Masao et al., 2015). The area is covered with a complex vegetation structure ranging from montane forest and tussock grassland in the highlands to semi-arid woodlands and short grasslands in the lowlands (Masao et al., 2015). The geology of the area is influenced by volcanism and tectonic movements, which are the active processes from the north-south of the East African Rift Valley system. The system is responsible for the formation of landscapes in the northern part and the Lake Manyara basin in the southern part of the study area (Żaba and Gaidzik, 2011b).

### 2.2. Data acquisition, quality control, and validation

#### 2.2.1. Observation data and quality control

Historical daily rainfall, maximum and minimum temperature, and observed station data from 1982 to 2011 for four climate stations of Arusha, Babati, Enduleni, and Ngorongoro were obtained from the Tanzania Meteorological Authority (TMA). Data quality control was performed on the four climate stations to select the meteorological station with data gaps not exceeding 10% of the study period (Larbi et al., 2018, Nkiaka et al., 2017, Westberg et al., 2013). Only the Arusha station passed this quality assurance test for rainfall and temperature data.

Due to the historical data limitations and uneven spatial distribution of climate stations at the catchment, satellite-based rainfall and temperature data were also used. The satellite rainfall data was taken from the Climate Hazards Group InfraRed Precipitation with Station (CHIRPS). The satellite temperature data was taken from the MERRA-2 of the National Aeronautics and Space Administration of Worldwide Energy Resource (NASA POWER) project. In all, fourteen gridded daily rainfall point data from CHIRPS and MERRA-2 maximum and minimum temperature data from NASA POWER for the period of 1982-2011 were extracted. The CHIRPS rainfall data is a product of the United States Geological Survey (USGS); and the University of California Santa Barbara (UCSB), with 0.05° spatial resolution (Funk et al., 2015). For the maximum and minimum temperature, 0.5° spatial resolution MERRA-2 data obtained from the NASA POWER (Westberg et al., 2013) project were used.

#### 2.2.2. CHIRPS rainfall and MERRA data validation

In order to validate the applicability of the satellite-based climate products (i.e. CHIRPS rainfall and MERRA-2), a comparison was made between the satellite-based data extracted for Arusha with historical daily rainfall and temperature data from the Arusha station. The Arusha station data was used for validation because Arusha was the only station in the vicinity of the study area with less than 10% data gap. The validation for the CHIRPS rainfall and MERRA-2 maximum and minimum temperature was performed for the period of 1982-2011 on a daily, monthly, and seasonal scale. Three standard valuation indices were used namely: (1) Nash–Sutcliffe efficiency (NSE), which compares the magnitude of the residual variance relative to that of the measured data variance using normalized statistics; (2) Percent bias (PBIAS), which measures the average tendency of the simulated data (larger or smaller) than the observed; and (3) the RMSE observations' standard deviation ratio (RSR), which standardizes the RMSE with regards to the observed records (Moriasi et al., 2015).

**Table 1**
NCEP predictors used during the screening process.

| S/N | Predictors | S/N | Predictors |
|---|---|---|---|
| 1 | Mean sea level pressure | 14 | 500 hPa divergence |
| 2 | 1000 hPa wind speed | 15 | 850 hPa wind speed |
| 3 | 1000 hPa zonal velocity | 16 | 850 hPa zonal velocity |
| 4 | 1000 hPa meridional velocity | 17 | 850 hPa meridional velocity |
| 5 | 1000 hPa vorticity | 18 | 850 hPa vorticity |
| 6 | 1000 hPa wind direction | 19 | 850 hPa geopotential height |
| 7 | 1000 hpa divergence | 20 | 850 hPa wind direction |
| 8 | 500 hPa wind speed | 21 | 850 hPa divergence |
| 9 | 500 hPa zonal velocity | 22 | Total precipitation |
| 10 | 500 hPa meridional velocity | 23 | 500 hPa specific humidity |
| 11 | 500 hPa relative vorticity | 24 | 850 hPa specific humidity |
| 12 | 500 hPa geopotential height | 25 | 1000 hPa specific humidity |
| 13 | 500 hPa wind direction | 26 | Air temperature at 2 m |

#### 2.2.3. NCEP and CanESM predictors for statistical downscaling

In the present study, twenty-six predictors (Table 1) from the National Centre for Environmental Prediction (NCEP) covering the historical period (1961-2005) were used (Gebrechorkos et al., 2019, Gulacha and Mulungu, 2017). The second-generation Canadian Earth System Model (CanESM2) predictors for RCP4.5 and RCP8.5 scenarios for the future (2006- 2050) with a spatial resolution of 2.81° were used for downscaling of the future rainfall and temperature. The selected scenarios have been principally used to run different models for the analysis based on medium- and high-range emission scenarios.

#### 2.2.4. Regional Climate Models (RCMs) dataset

RCMs datasets (Table 2) at 50 km resolution from the CORDEX-Africa experiment were used for this study. The four CORDEX-Africa RCMs (REMO2009, CanESM2-RCA4, NorESM1-RCA4 and KNMI-RACMO22T) are downscaled dynamically from GCMs. The RCM datasets used in this study at daily scale consist of rainfall, minimum and maximum temperature for the RCM historical (1981–2005) and RCP4.5 and 8.5 projected (2021–2050) period. These RCMs were chosen because they were found to perform well over the sub- region with acceptable range of biases (López-Moreno et al., 2011, Larbi et al., 2021, Kim et al., 2013). It is worth mentioning that the RCMs covers about 23 grid boxes over the study area (Fig. 1c).

### 2.3. Statistical downscaling

#### 2.3.1. Statistical downscaling of GCM outputs using SDSM

The SDSM is designed to statistically downscale simulated climate information from either coarse-resolution GCM output or large at-

**Table 2**
Description of the Regional Climate Models used in this study.

| S/N | Institute | Forcing GCM. | RCMs |
|---|---|---|---|
| 1 | Swedish Meteorological and Hydrological Institute, Rossby Centre (SMHI) | CCCma-CanESM2 CNRM-CERFACS- CM5 NCC-NorESM1-M | CanESM2-RCA4 and NorESM1-RCA4 |
| 2 | Max Planck Institute- Computational methods in systems and control theory (MPI-CSC), Germany | ICHEC-ECEARTH | REMO2009 |
| 3 | Koninklijk Nederlands Meteorologisch Instituut (KNMI) | ICHEC-ECEARTH | KNMI-RACMO22T |

mospheric variables to high-resolution forms needed for local impact studies using predictors and predictands (Gebrechorkos et al., 2019, Luhunga et al., 2018). The SDSM uses multivariate linear regression to simulate future climate scenarios by combining stochastic weather generator and transfer function models (Wilby et al., 2002). The stochastic data was included in the SDSM to improve the model's performance in reproducing the observed daily series by inflating the model output variance (Wilby et al., 2002). In the present study, the SDSM was applied in the watersheds around the NCA to downscale the CanESM daily rainfall and temperature to point-scale. Two datasets were involved in this process: 1) the predictands of interest i.e., locally observed rainfall and temperature and the corresponding large-scale predictors from NCEP and CanESM2 in the study area's grid box (Shukla et al., 2016). Model calibration and respective downscaling were performed through the following steps as suggested by Wilby et al. (Wilby et al., 2002):

1 Screening of the 26 large-scale NCEP predictors based on the correlation matrix, partial correlation, and *p*-value indicators between the predictors and local-scale predictands as practiced in previous studies (Gebrechorkos et al., 2019, Gulacha and Mulungu, 2017). Highly correlating predictors at a 95% confidence level ($p$-value < 0.05) were selected. For regression analysis between the selected NCEP predictors and predictands during model calibration for each station, a minimum of three large-scale variables was recommended for calibration at each station (Gebrechorkos et al., 2019, Huang et al., 2011).
2 The SDSM model calibration and validation were performed for the periods of 1982-1996 and 1997-2005, respectively, under 'conditional' for the rainfall and 'unconditional' for the temperature on a monthly scale. Several studies have applied this method of splitting the data into two for SDSM calibration and validation, such as (Gebrechorkos et al., 2019, Gulacha and Mulungu, 2017, Osman and Abdellatif, 2016) with SDSM indicating satisfactory results.
3 Generation of daily synthetic data series for rainfall, maximum and minimum temperatures for the period of 1982-2005 was performed by the weather generator (WG) using the calibrated SDSM. The WG was applied to produce the weather series with similar statistical properties to those of the observed location-based data (Li and Babovic, 2019).
4 The SDSM performance was evaluated using statistical indicators including Nash-Sutcliffe efficiency (NSE), Percent bias (Pbias), and RMSE observation's standard deviation ratio (RSR), which were also used to evaluate the SDSM performance at a daily, monthly, and seasonal timescale.

The model scenario generator, which follows a similar process as step (3), was applied to downscale the CanESM2 daily rainfall and temperature for the future period of 2006-2050 under RCP4.5 and RCP8.5 scenarios.

#### 2.3.2. Statistical downscaling of GCM outputs using LARS-WG

LARS-WG is a stochastic weather generator designed to simulate the daily climate data at a station scale for climate change impact studies (Semenov and Barrow, 2002, Chen et al., 2013). The LARS-WG synthesizes daily series data through three processes;

1 The LARS-WG use statistical properties of the station data on a monthly scale to generate the probability distribution of the climate parameters for a particular station on the ground.
2 LARS-WG use the generated parameters files to synthesize data with the same statistical properties as the station data. Furthermore, observed and simulated average monthly weather statistical indices calibrate LARS-WG using calculated relative change factors from the GCMs outputs for each month.
3 Finally, LARS-WG uses the calibrated parameters and relative change factors to project daily time-series data (Semenov and Barrow, 2002, Chen et al., 2013).

This study applied LARS-WG6 to downscale rainfall and temperature for each station individually by incorporating 20 years (1982-2001) to generate model calibration parameters. For model validation, a ten-year extended time series (2002-2011) was generated and examined using a statistical test at a 5% significance level to determine the significant difference between the simulated and observed data. After the calibration and validation process of LARS-WG, the model generated future weather data series by updating model output parameters with selected RCMs and RCPs. This study applied LARS-WG to downscale rainfall and temperature data series for future 2021-2050 from four GCMs (CanESM2-RCA4, NorESM1-RCA4, CSIRO-CMS and HadGEM2-ES) under RCP 4.5 and 8.5.

### 2.4. RCMs models performance evaluation and climate change analysis

The performances of the raw CORDEX-Africa RCMs (REMO2009, CanESM2-RCA4, NorESM1-RCA4, and KNMI-RACMO22T) in simulating the observed climatology over the study area were evaluated at monthly and annual scale for the period 1982-2005 using statistics such as Pearson correlation (r), Nash-Sutcliff Efficiency (NSE) and percentage bias (PBIAS). The r represents the temporal pattern of the models. The PBIAS describes the relative systematic error associated with the CMIP 6 models' data, where a positive and negative sign indicate overestimation and underestimation respectively. At the spatial scale, the biases between the models and the observation were also estimated using the PBIAS statistical indicator.

Temporal and spatial changes in rainfall and temperature at annual and seasonal scale for the observed historical period of 1982-2011, and the future periods of 2021-2050 were analyzed using the ensemble mean of four (4) RCMs and five (5) statistically downscaled GCMs outputs. The percentage changes in rainfall at seasonal and annual scales and the projected relative changes in the mean annual temperature were estimated for each station and over the entire basin. The significance of the projected changes was assessed at a 95% confidence level using the *t*-test. For the spatial analysis, the Inverse Distance Weighted (IDW) interpolation method was used to generate the distribution of seasonal and mean annual change in rainfall and temperature between the future and historical period.

## 3. Results

### 3.1. Validation of CHIRPS and MERRA-2 data

The statistical results of CHIRPS rainfall data showed NSE = 0.51, Pbias = -16.10, and RSR = 0.68 at the daily timescale and NSE = 0.78, Pbias = -8.2, and RSR = 0.46 at the monthly timescale. Therefore, CHIRPS rainfall data for the Arusha station compares very well with observation data at monthly timescales. Also, validation for the MERRA-2 data for the Arusha station showed a good agreement with the observation data at a daily and monthly timescale for both maximum and minimum temperature. The statistics indicated that NSE = 0.82, Pbias = -13.7, and RSR = 0.58 for the maximum temperature and NSE = 0.93, Pbias = -12.7, and RSR = 0.39 for the minimum temperature for a daily timescale. For the monthly timescale, the indices showed that NSE = 0.88, Pbias = -8.4, and RSR = 0.54 for the maximum temperature and NSE = 0.96, Pbias = -14.4, and RSR = 0.48 for the minimum temperature.

### 3.2. Performance evaluation statistics of RCMs over the catchment

The statistical tests for comparison between the observation and the RCMs (REMO2009, CanESM2-RCA4, NorESM1-RCA4, and KNMI-RACMO22T) in simulating the rainfall and temperature for the period 1982 to 2005 is presented in Table 3. High correlation (r) greater than 0.9 was found for all the RCMs for rainfall and Temperature. Three of the

**Table 3**
Statistical analysis between the raw RCMs and observation for the mean monthly rainfall and temperature of the catchment for the period 1981-2005.

| Models | Rainfall | | | Temperature | | |
|---|---|---|---|---|---|---|
| | r | PBIAS | NSE | r | BIAS | NSE |
| REMO2009 | 0.96 | 13.0 | 0.86 | 0.97 | 1.4 | 0.88 |
| CanESM2-RCA4 | 0.92 | 16.0 | 0.71 | 0.94 | 0.8 | 0.75 |
| NorESM1-RCA4 | 0.9 | -2.5 | 0.95 | 0.92 | 0.2 | 0.91 |
| KNMI-RACMO22T | 0.94 | 16.7 | 0.84 | 0.95 | 0.9 | 0.81 |

Note: r indicates correlation; NSE indicates Nash-Sutcliffe Efficiency.

RCMs (REMO2009, KNMI-RACMO22T and CanESM2-RCA4) show overestimation of rainfall in the area in the range of 13% to 16.7%, while NorESM1-RCA4 shows underestimation of rainfall with PBIAS of -2.5%. A similar rainfall results of higher correlation between the RCMs and the observation was found for temperature. Unlike rainfall, all the RCMs show overestimation in the case of temperature with biases in the range of 0.2 to 1.4°C. In addition, Fig. 3 and 4, (a, b, c and d), respectively indicate the spatial biases between observed data and RCMs for rainfall and temperatures. The spatial PBIAS was found to range between +20.3% and -28.9% for rainfall. In the case of temperature, all the RCMs show overestimation with biases in the range of 0.01 to 1.98 °C. The biases across the basin found in NorESM1-RCA4 and KNMI-RACMO22T models were relatively low compared to REMO2009 and CanESM2-RCA4.

### 3.3. Screening of the predictors for statistical downscaling using the SDSM

The screening of suitable predictor variables is an important process in statistical downscaling. The power of each predictor is distinguishable in space and time, making the choice of predictors to differ according to the geographical location and the relationship between predictors and predictands to be downscaled. With reference to the coefficient of correlation (*r*) and partial correlation (partial-*r*), among the individual best performed NCEP predictors in the SDSM, the selected suitable predictors for downscaling of rainfall and temperatures are listed in Table 4.

**Table 4**
Selected predictor variables from NCEP.

| Parameter | Predictors | *r* | *p*-value | Partial-*r* |
|---|---|---|---|---|
| Rainfall(mm) | Mean sea level pressure | 0.38 | 0.0047 | 0.247 |
| | 850 hPa geopotential height | 0.36 | 0.0047 | 0.144 |
| | 1000 hPa specific humidity | 0.39 | 0.0081 | 0.281 |
| $T_{max.}$ ($^0$C) | Mean sea level pressure | 0.42 | 0.0000 | 0.180 |
| | 1000 hPa meridional velocity | 0.40 | 0.0000 | 0.381 |
| | 850 hPa geopotential height | 0.40 | 0.0000 | 0.325 |
| | Air temperature at 2 m | 0.50 | 0.0000 | 0.380 |
| $T_{min.}$ ($^0$C) | Mean se level pressure | -0.60 | 0.0000 | -0.137 |
| | 1000 hPa meridional velocity | -0.50 | 0.0008 | -0.239 |
| | 850 hPa geopotential height | 0.60 | 0.0000 | 0.503 |
| | 1000 hPa specific humidity | 0.60 | 0.0000 | 0.469 |
| | Air temperature at 2 m | 0.40 | 0.0000 | 0.297 |

### 3.4. Performance evaluation of the SDSM and LARS-WG outputs

#### 3.4.1. Perfomance of SDSM

The SDSM validation results for the simulated rainfall, maximum and minimum temperatures for all stations are shown in Tables 5, 6 and 7, respectively. The SDSM indicated poor performance in simulating the daily rainfall with Nash-Sutcliffe efficiency (NSE), Percent bias (Pbias), and RMSE observation's standard deviation ratio (RSR) ranging from 0.12 to 0.25, -56.30 to -26.10, and 0.63 to 0.87, respectively (Table 5). However, the model performed relatively well in reproducing maximum and minimum temperatures at the daily timescale (Tables 6 and 7). The model had NSE, Pbias, and RSR ranging from 0.70 to 0.89, -17.8 to 11.8 and 0.39 to 0.58, for the maximum temperature; 0.67 to 0.97, -17.8 to 7.8, and 0.35 to 0.59, for minimum temperature, respectively.

At monthly and seasonal timescales, the model performed well in simulating both rainfall and maximum and minimum temperatures. For rainfall at a monthly timescale, the model had NSE, Pbias, and RSR that

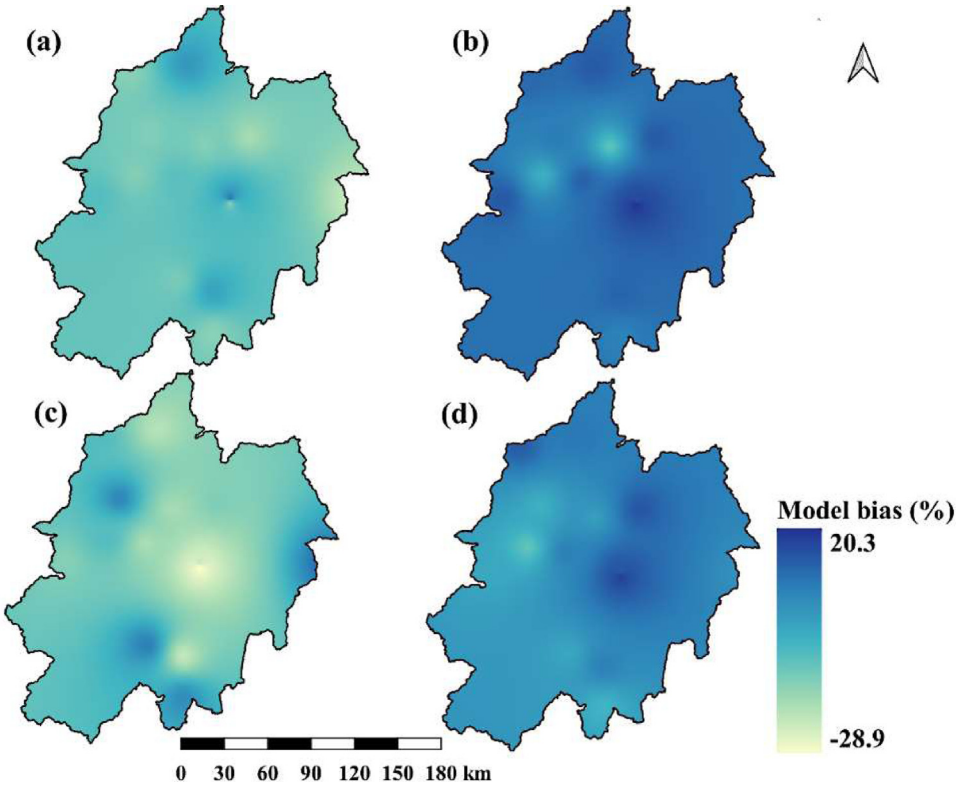


**Fig. 2.** Spatial biases for rainfall data between observed and CORDEX RCMs ((a). REMO2009, (b). CanESM2-RCA4, (c). NorESM1-RCA4 and (d). KNMI-RACMO22T).

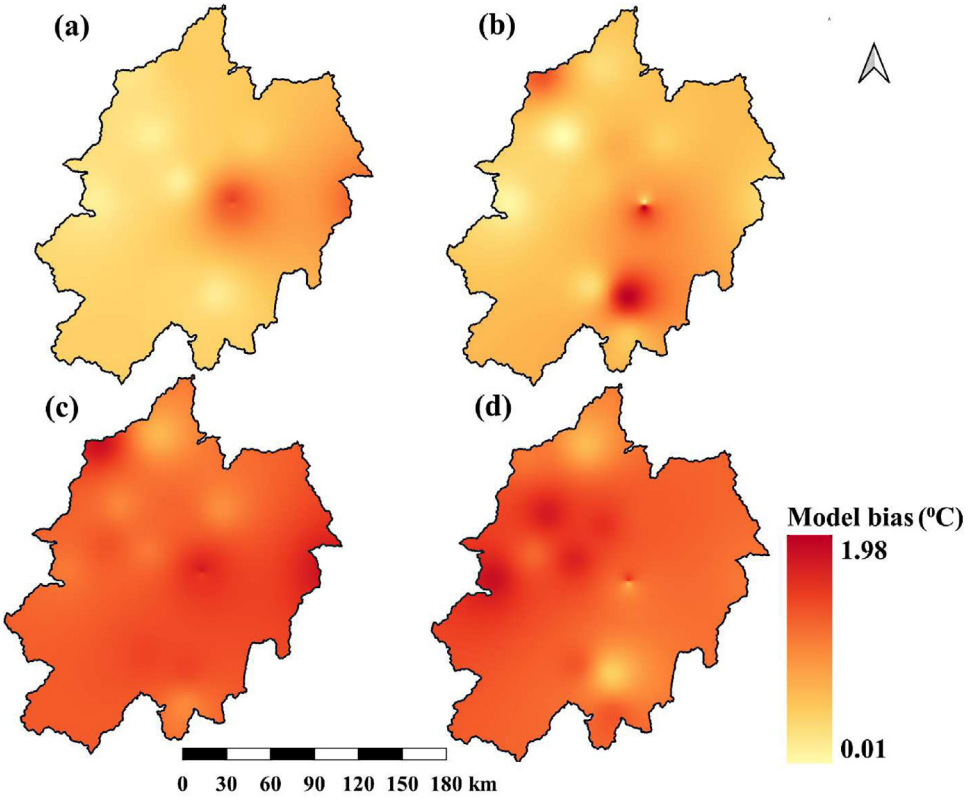


**Fig. 3.** Spatial biases (°C) for temperature data between observed and CORDEX RCMs ((a). REMO2009, (b). CanESM2-RCA4, (c). NorESM1-RCA4, and (d). KNMI-RACMO22T).

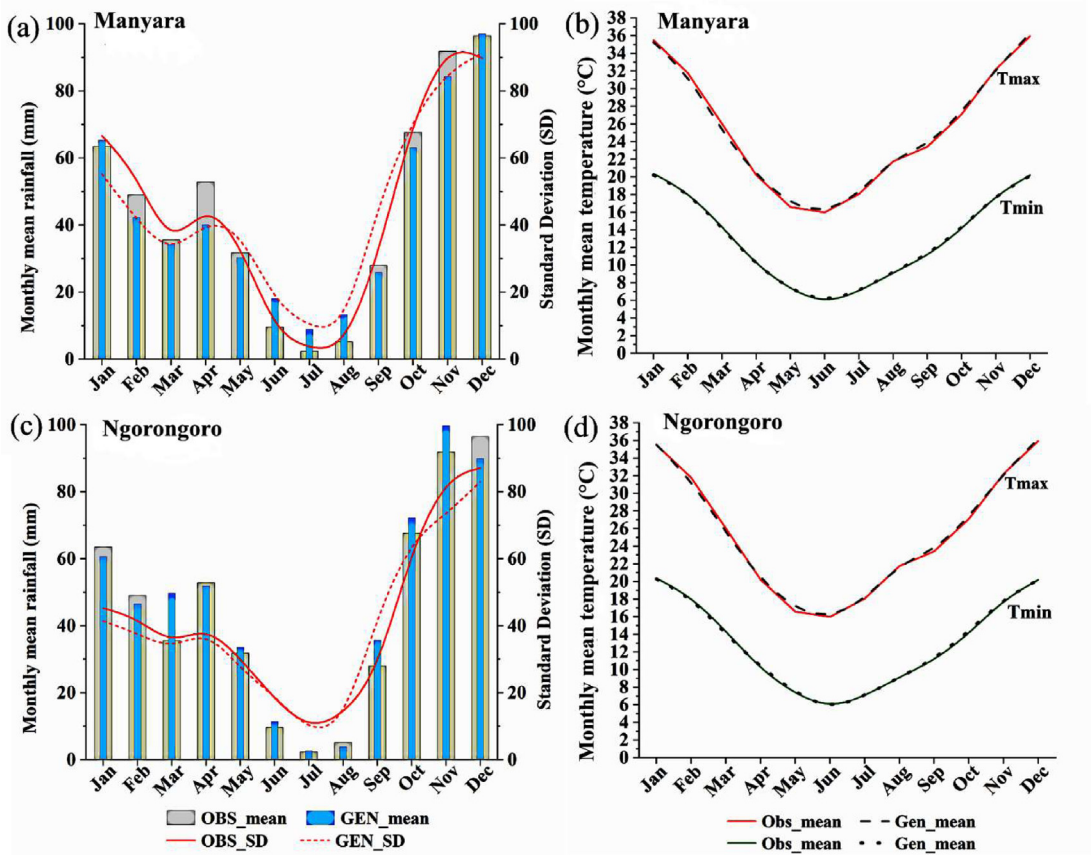


**Fig. 4.** Calibration of LARS-WG for mean monthly rainfall (mm) and temperatures for Manyara (a and b), and Ngorongoro (c and d), respectively.

**Table 5**
Model performance for the Rainfall (mm) simulation for daily, monthly, and seasonal timescales during the validation period of 1997- 2005.

| | | Daily | | | Monthly | | | Seasonal | | |
|---|---|---|---|---|---|---|---|---|---|---|
| S/N | Station | NSE | Pbias | RSR | NSE | Pbias | RSR | NSE | Pbias | RSR |
| 1 | Arusha | 0.24 | -26.10 | 0.68 | 0.98 | -4.40 | 0.10 | 0.78 | -6.40 | 0.54 |
| 2 | Babati | 0.18 | -28.30 | 0.87 | 0.88 | -13.80 | 0.57 | 0.97 | -11.80 | 0.48 |
| 3 | Enduleni | 0.22 | -34.60 | 0.73 | 0.95 | -1.60 | 0.05 | 0.95 | -9.60 | 0.42 |
| 4 | Engaruka | 0.25 | -27.20 | 0.68 | 0.94 | -0.70 | 0.06 | 0.79 | -10.70 | 0.58 |
| 5 | Idulu | 0.16 | -29.50 | 0.72 | 0.97 | -0.90 | 0.04 | 0.99 | -5.90 | 0.34 |
| 6 | Kakesio | 0.23 | -32.70 | 0.86 | 0.76 | 0.80 | 0.04 | 0.91 | 1.80 | 0.51 |
| 7 | Manyara | 0.18 | -56.30 | 0.74 | 0.88 | -12.30 | 0.45 | 0.94 | -13.20 | 0.33 |
| 8 | Mbulu | 0.21 | -27.20 | 0.63 | 0.90 | -13.30 | 0.96 | 0.64 | -12.30 | 0.52 |
| 9 | Mto'Mbu | 0.24 | -35.60 | 0.67 | 0.83 | 1.70 | 0.06 | 0.91 | 1.90 | 0.57 |
| 10 | Nainokanoka | 0.15 | -44.20 | 0.72 | 0.76 | -1.20 | 0.05 | 0.83 | -4.20 | 0.39 |
| 11 | Ndutu | 0.24 | -32.40 | 0.77 | 0.86 | -1.20 | 0.05 | 0.62 | -7.20 | 0.51 |
| 12 | Ngorongoro | 0.22 | -47.30 | 0.81 | 0.91 | -12.10 | 0.16 | 0.81 | -11.10 | 0.56 |
| 13 | Olala | 0.12 | -28.20 | 0.70 | 0.86 | -9.30 | 0.08 | 0.77 | -8.30 | 0.44 |
| 14 | Olduvai | 0.20 | -31.60 | 0.68 | 0.82 | -3.20 | 0.58 | 0.83 | -2.70 | 0.36 |

**Table 6**
Model performance for the maximum temperature ($^0$C) simulation for daily, monthly, and seasonal timescales during the validation period of 1997- 2005.

| | | Daily | | | Monthly | | | Seasonal | | |
|---|---|---|---|---|---|---|---|---|---|---|
| SN | Station | NSE | Pbias | RSR | NSE | Pbias | RSR | NSE | Pbias | RSR |
| 1 | Arusha | 0.82 | -13.70 | 0.58 | 0.88 | -8.40 | 0.54 | 0.81 | -11.05 | 0.52 |
| 2 | Babati | 0.87 | -17.80 | 0.48 | 0.78 | -14.60 | 0.53 | 0.83 | -14.20 | 0.58 |
| 3 | Enduleni | 0.75 | -12.60 | 0.52 | 0.85 | -11.60 | 0.49 | 0.84 | -12.10 | 0.59 |
| 4 | Engaruka | 0.89 | -14.70 | 0.57 | 0.95 | -6.70 | 0.52 | 0.86 | -10.70 | 0.47 |
| 5 | Idulu | 0.79 | -15.90 | 0.44 | 0.93 | -10.90 | 0.64 | 0.79 | -13.40 | 0.58 |
| 6 | Kakesio | 0.81 | 11.80 | 0.51 | 0.86 | 6.80 | 0.48 | 0.83 | 9.30 | 0.54 |
| 7 | Manyara | 0.84 | -14.20 | 0.39 | 0.78 | -14.30 | 0.42 | 0.81 | -14.25 | 0.56 |
| 8 | Mbulu | 0.74 | -10.30 | 0.55 | 0.82 | -11.60 | 0.62 | 0.78 | -10.95 | 0.50 |
| 9 | Mto'Mbu | 0.81 | 7.90 | 0.47 | 0.81 | 11.30 | 0.57 | 0.79 | 9.60 | 0.51 |
| 10 | Nainokanoka | 0.87 | -6.20 | 0.49 | 0.78 | -13.20 | 0.47 | 0.85 | -9.70 | 0.54 |
| 11 | Ndutu | 0.72 | -5.20 | 0.56 | 0.96 | -9.20 | 0.51 | 0.82 | -7.20 | 0.54 |
| 12 | Ngorongoro | 0.77 | -12.10 | 0.51 | 0.94 | -12.70 | 0.44 | 0.80 | -12.40 | 0.49 |
| 13 | Olala | 0.70 | -6.30 | 0.54 | 0.88 | -10.30 | 0.61 | 0.92 | -8.30 | 0.41 |
| 14 | Olduvai | 0.73 | -12.70 | 0.47 | 0.84 | -13.40 | 0.57 | 0.86 | -13.05 | 0.58 |

**Table 7**
Model performance for the minimum temperature ($^0$C) simulation on the daily, monthly, and seasonal timescale during the validation period of 1997- 2005.

| | | Daily | | | Monthly | | | Seasonal | | |
|---|---|---|---|---|---|---|---|---|---|---|
| SN | Station | NSE | Pbias | RSR | NSE | Pbias | RSR | NSE | Pbias | RSR |
| 1 | Arusha | 0.93 | -12.70 | 0.39 | 0.96 | -14.40 | 0.48 | 0.81 | -13.55 | 0.44 |
| 2 | Babati | 0.97 | -15.80 | 0.57 | 0.94 | -9.60 | 0.56 | 0.83 | -12.70 | 0.56 |
| 3 | Enduleni | 0.86 | -11.60 | 0.45 | 0.88 | -10.80 | 0.51 | 0.84 | -11.20 | 0.48 |
| 4 | Engaruka | 0.82 | -12.70 | 0.59 | 0.84 | -15.10 | 0.53 | 0.86 | -13.90 | 0.56 |
| 5 | Idulu | 0.89 | -10.90 | 0.47 | 0.82 | -8.90 | 0.56 | 0.79 | -9.90 | 0.52 |
| 6 | Kakesio | 0.91 | 7.80 | 0.43 | 0.81 | 9.60 | 0.48 | 0.83 | 8.70 | 0.46 |
| 7 | Manyara | 0.88 | -11.20 | 0.49 | 0.78 | -9.70 | 0.49 | 0.81 | -10.45 | 0.49 |
| 8 | Mbulu | 0.76 | -14.30 | 0.35 | 0.96 | -7.20 | 0.49 | 0.78 | -10.75 | 0.42 |
| 9 | Mto'Mbu | 0.71 | 5.90 | 0.48 | 0.94 | -12.40 | 0.52 | 0.79 | -3.25 | 0.50 |
| 10 | Nainokanoka | 0.77 | -13.30 | 0.59 | 0.84 | -10.70 | 0.53 | 0.85 | -12.00 | 0.56 |
| 11 | Ndutu | 0.82 | -7.20 | 0.46 | 0.86 | -13.40 | 0.50 | 0.82 | -10.30 | 0.48 |
| 12 | Ngorongoro | 0.67 | -13.10 | 0.52 | 0.79 | -12.30 | 0.48 | 0.80 | -12.70 | 0.50 |
| 13 | Olala | 0.90 | -12.30 | 0.44 | 0.83 | -11.25 | 0.49 | 0.92 | -11.78 | 0.46 |
| 14 | Olduvai | 0.78 | -11.70 | 0.39 | 0.81 | -10.40 | 0.51 | 0.86 | -11.05 | 0.45 |

ranged from 0.76 to 0.98, -13.8 to 1.70, and 0.04 to 0.58, respectively. For the maximum and minimum temperatures at a monthly timescale, the model performance showed NSE, Pbias and RSR ranging from 0.78 to 0.96, -14.60 to 11.30, and 0.42 to 0.64; and 0.78 to 0.96, -15.10 to 9.60, and 0.48 to 0.56, respectively. Besides, the model performed well in simulating rainfall, maximum and minimum temperatures at a seasonal scale. The model performance showed NSE, Pbias, and RSR ranging from 0.62 to 0.99, -13.20 to 1.90, and 0.33 to 0.61; 0.78 to 0.92, -16.20 to 9.60, and 0.41 to 0.59; and 0.78 to 0.92, -13.90 to 8.70 and, 0.42 to 0.58, respectively, for the rainfall, maximum temperature, and minimum temperature. Therefore, for monthly and seasonal timescales the SDSM could be used as tool to simulate rainfall data. Moreover, the model simulated temperature data with good precision for daily, monthly, seasonal timescales.

**Table 8**
Model performance for the rainfall (mm) Maximum temperature ($^0$C) and minimum temperature ($^0$C) at a daily and monthly timescale during the validation period of 2002 -2011 for the entire basin.

| Scale | Parameter | NSE | RSR | RMSE | Pbias | $R^2$ |
|---|---|---|---|---|---|---|
| Daily | Rainfall | -0.80 | 1.34 | 7.94 | -1.10 | 0.00 |
| | Tmax | -0.70 | 1.30 | 10.05 | 14.90 | 0.52 |
| | Tmin | 0.89 | 1.38 | 8.05 | 26.20 | 0.47 |
| Monthly | Rainfall | 0.78 | 0.81 | 14.58 | -8.50 | 0.53 |
| | Tmax | -0.80 | 1.29 | 9.15 | 15.10 | 0.64 |
| | Tmin | -1.15 | 1.41 | 7.43 | 26.5 | 0.91 |

### 3.4.2. Performance of LARS-WG in statistical downscaling of GCMs

The LARS-WG performance are shown in Fig. 4 (calibration) and Table 8 (validation). Fig. 4a and c indicate the monthly mean rainfall and standard deviations of the synthesized by LARS-WG data compared to the observed data during calibration period (1982-2001). However, Fig. 4 (b and d) indicates the comparison between observed and synthesized monthly mean maximum and minimum temperature. Results indicate good performance of the LARS-WG to synthesize data series with similar characteristics of the observed data. Furthermore, the statistical test to validate the LARS-WG output was performed and indicated in Table 8.

## 3.5. Projected climate change under RCP4.5 and RCP8.5 scenarios

### 3.5.1. Spatial-temporal changes in rainfall

Percentage changes in the mean seasonal (JF, MAM, JJAS, and OND), and annual rainfall for the future (2021-2050) period under RCP 4.5 and RCP 8.5 scenarios compared to the historical (1982-2011) period at the temporal scale are presented in Fig. 5. The rainfall data shows an increase in all seasons except the JJAS season that shows a decrease of 13 and 16% under RCP 4.5 and RCP 8.5, respectively. The annual rainfall indicates an increase with an average of 4% under RCP4.5 and 5% under RCP 8.5.

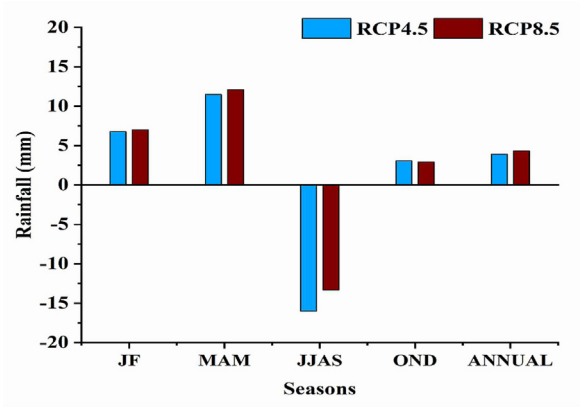


**Fig. 5.** Percentage change in seasonal and annual mean rainfall for the future period (2021-2050) under RCP 4.5 and RCP 8.5, compared to the simulated historical period (1982-2011).

The spatial distribution of the changes in annual rainfall for 2021-2050 under RCP4.5 and RCP8.5 are depicted in Fig. 6a-b. Spatially, the rainfall would increase over the entire study area during the period of 2021-2050 under both RCPs, with the highest increase over the Eastern, Southern parts and some areas in the West. The central, western and northern parts of the study area would experience a low percentage increase in rainfall with the lowest percentage of 2 % under both RCPs. Both RCPs indicates similar patterns over the area for the future 2021-2050, however RCP 4.5 outputs show higher increases compared to the RCP 8.5.

### 3.5.2. Projected changes in temperature

The annual maximum, minimum and mean temperature change under RCPs 4.5 and 8.5 are presented in Table 9. The results indicate an increase in maximum, minimum, and mean temperature, respectively by 0.4˚C, 0.6˚C, and 0.5˚C under RCP 4.5 and 0.6˚C for both maximum,

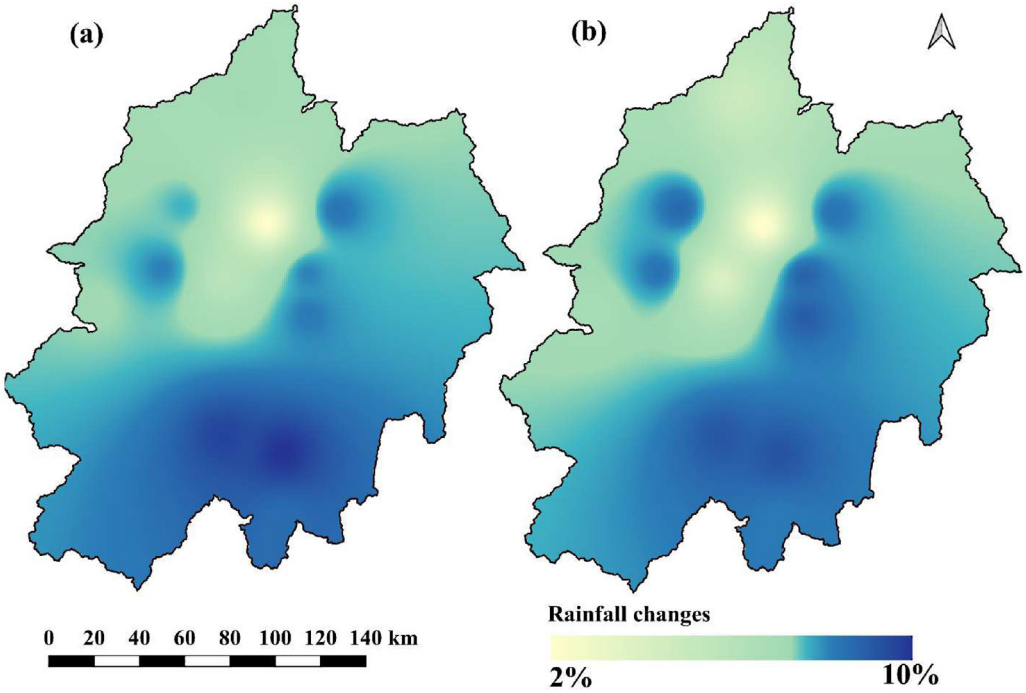


**Fig. 6.** Spatial distribution of changes in the mean annual rainfall under RCP4.5 (a) and RCP8.5 (b) for the period of 2021-2050 compared to the historical period of 1982-2011.

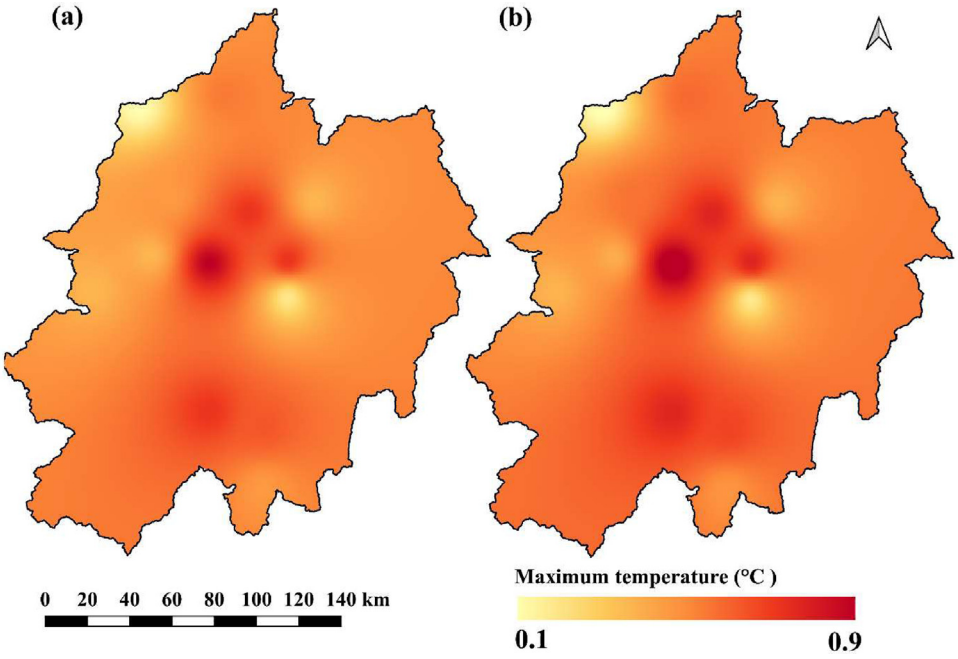


**Fig. 7.** Spatial distribution for the annual maximum temperature anomalies (°C) under RCP4.5 (a) and RCP8.5 (c) for the period of 2021-2050 compared to the historical period of 1982-2011.

**Table 9**
Temperature (°C) projections and change signal for the (2021-2050) future under RCP4.5 and RCP8.5 scenarios relative to the historical (1982-2011) period the ensemble mean.

| Temperature | Historical (1982-2011) | RCP4.5 scenario | RCP8.5 scenario |
|---|---|---|---|
| Maximum | 26.9 | 27.3 (+0.4) * | 27.5 (+0.6) * |
| Minimum | 14.3 | 14.8 (+0.6) * | 14.9 (+0.5) * |
| Mean | 20.6 | 21.1 (+0.5) * | 21.1 (+0.6) * |

Values in brackets indicate the projected changes.
* Indicates the significance of the projected changes at a 95% confidence level.

minimum and mean temperature under RCP 8.5 during the future 2021-2050 as captured by the ensemble mean.

### *3.5.3. Spatial distribution of temperature change*

Spatial distribution for the maximum and minimum temperature change for the future periods of 2021-2050 under RCP4.5 and RCP8.5 emission scenarios as captured by the SDSM and RCMs ensembles are presented in Fig. 7 a-b and Fig. 8 a-b, respectively. The results for the maximum temperature change indicate warming over the study area with spatial variations. The maximum temperature increases during the period of 2021-2050 is expected to be in the range of 0.1 to 0.8°C under RCP 4.5. The highest increase is at the central and southern parts and the lowest increase over the western and northwestern areas and few parts in the east of the study area. The maximum temperature rises for the same period, under RCP8.5, would be between 0.1°C and 0.9°C, with the highest value in the central and the southern parts, most of the areas would be warmer by a range of 0.2°C to 0.8°C during the 2021-2050 period under both RCPs as captured in (Fig. 7 (a-b).

The results for the minimum temperature change (8 (a-b)) also show a warming regime over the study area with variations in spatial distribution. The minimum temperature rises during 2021-2050 is expected to range from 0.1°C to 1.0°C, under RCP4.5. The highest increases are in the central and south of the study area while northwestern areas and part of the central area would experience the lowest rise as captured by the ensemble mean of LARS-WG, SDSM and RCMs. The minimum temperature rises for the same period, under RCP8.5, would be between 0.1 and 0.9°C, with the highest value covering a large part of the central and south, of the study area and the lowest found in the northwestern areas and parts of central areas. Generally, most of the areas would be anomalously warmer by 0.2°C to 0.8°C under both RCPs as shown in Fig. 8 (a-b).

## 4. Discussion

The present study applied the CORDEX RCMs, SDSM and LARS-WG ensembles to analyze the change in climate around the NCA by comparing the future projection for the periods of 2021-2050 with historical data from the period of 1982-2011. Using the obtained information, the study determined the potential climatic impacts and adaptation measures. The validation of CHIRPS rainfall and MERRA-2 maximum and minimum temperature at the point-scale performed very well compared with the observation data from the Arusha station. Although as shown in previous studies (Larbi et al., 2018, Molua, 2009), there is a relatively weaker agreement between CHIRPS rainfall and surface measurements at a daily timescale. However, for areas with no observed data, the high accuracy data acquired from remote sensing, followed by reanalysis, can be used in place of the observation data (Gebrechorkos et al., 2019, Gebrechorkos et al., 2018). Therefore, for this analysis, CHIRPS rainfall and MERRA-2 maximum and minimum temperature data at point-scale were used.

The results of the SDSM model evaluation showed a high capability in downscaling the CanESM2 global climate model datasets (i.e., rainfall and temperature) for climate projections in the watersheds surrounding the NCA of Northern Tanzania at the monthly and annual scales. The weak correlation between NCEP and CanESM2 data for the daily rainfall can be attributed to the fact that the SDSM model calibration and validation were performed under 'conditional' for the rainfall and 'unconditional' for the temperature on a monthly scale. In the SDSM, the model type used for SDSM calibration is at monthly, seasonal or annual scales but not at daily scale. As a result of this, the predictand and predictors relationships are established at the monthly scale but not at the daily scale. Hence the reason why the SDSM model performs poorly at the daily scale for rainfall but performs well at monthly scale. Additionally, different studies have recognized the high performance of SDSM at the monthly or annual scale, and also as a tool for filling data gaps over data-scarce regions of Africa (Gebrechorkos et al., 2018, Moriasi et al., 2015). For Example, (Bessah et al., 2021) obtained a good model

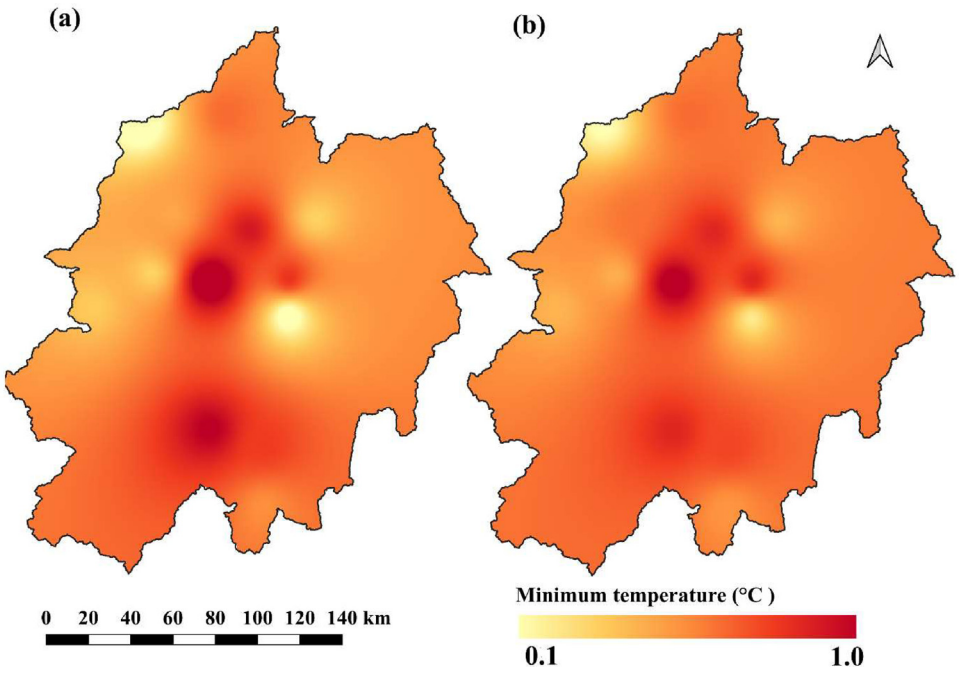


**Fig. 8.** Spatial distribution for the annual minimum temperature anomalies (°C) under RCP4.5 (a) and RCP8.5 (c) for the period of 2021-2050 compared to the historical period of 1982-2011.

accuracy with Nash–Sutcliffe efficiency (NSE), percent bias (PBIAS) and RMSE observations standard deviation ratio (RSR) in the range of 0.80–0.98, (-21.7) – (+0.26) and 0.11–0.45, respectively. This is also in line with the findings from this study which has demonstrated the usefulness of SDSM in modelling at monthly and seasonal scales with high accuracy. Furthermore, considering the difficulties in modelling climate variables, especially precipitation, due to factors such as the complex local topography, and also unavailability of climate data at the study region, the model results of the present study can be useful for climate impact assessment studies.

The evaluation results of CORDEX RCMs (REMO2009, CanESM2-RCA4, NorESM1-RCA4, and KNMI-RACMO22T) indicate good performance of the RCMs in simulating monthly rainfall and temperatures as shown in Table 2. Similarly, the Four GCMs (i.e. CanESM2-RCA4, NorESM1-RCA4, CSIRO-CMS and HadGEM2-ES) used to generate daily rainfall and temperature data for RCP 4.5 and 8.5 using the LARS-WG model shows good performance in synthesizing data series at a daily and monthly time scale for the entire basin during validation period as indicated in Table 8 and Fig. 7. These results are in consistence with other studies [e.g., 36, 37] which indicated a good performance of LARS-WG in generating daily and monthly rainfall and temperature data.

The comparison between future projections and the historical data showed increasing rainfall for all seasons except JJAS, which showed a decreasing trend for both RCPs. However, the annual rainfall showed a significantly increasing pattern for the periods of 2021-2050 for both RCPs. Likewise, for the maximum and minimum temperatures, the annual increase in temperature would occur during the future periods, with a higher rise predicted under RCP8.5. The results agree with other studies in Tanzania (Cooper et al., 2008, Luhunga et al., 2018, Mtongori et al., 2016, Wambura et al., 2014b), which predicted an increase in rainfall over the northeastern highlands of Tanzania. The results are also consistent with other previous studies (Luhunga et al., 2018, Wambura et al., 2014b), that showed an increase in maximum and minimum temperature for all future periods and RCPs but with the highest rise under RCP8.5. Spatially, the highest increase in rainfall would generally occur from the central to the southern parts of the study area for all future periods under both RCPs. For the maximum temperature, the highest rise would occur over the central and southern parts of the study area under RCP4.5 and extended to the northeastern parts under RCP8.5 for both future periods. For the minimum temperature, almost all the study areas would feature increases with a high rise from the center towards the western and eastern parts for both RCPs.

As previously reported, the projected rise in rainfall and temperature can affect water resources, their services, and the prevalent enviro-social-economic activities in the study area (IPCC 2007, IPCC 2012, IPCC 2014, Obuobie et al., 2012). The Government of Tanzania has reported climate change impacts in several places, including in the protected areas of conservation importance (United Republic of Tanzania 2008). The Government has shown concerns about the increase in the frequency of drought and flood events in its protected areas. The severity of climatic events has led to encroachment problems to local communities where communities are increasingly forced to expand their activities into conserved areas. The present study's projected increase in rainfall and temperature raises further concerns for the NCA and its surrounding ecosystems. The projected increase in rainfall in the present study agrees with the findings of (Donat et al., 2016) who projected that the world's dry places like the tropics would experience more extreme precipitation. The projected increase in rainfall has the advantage of a constant water supply to the biodiversity and ensuring food security to the expanding human population in the Ngorongoro Conservation Area and its surroundings.

(Tarver et al., 2019) have recounted that the NCA is one of the essential conservation areas for wildlife tourism and ecotourism in Tanzania, where a harmonious relationship between wildlife, people, and livestock exists. Regrettably, the projected increase in rainfall and the corresponding increase in temperature would significantly impact the hydrological patterns of this UNESCO world heritage site, resulting in natural hazards such as frequent flooding and droughts (Sayasane et al., 2016, Serdeczny et al., 2016, Shemsanga et al., 2010). Furthermore, an increase in temperatures enhances evapotranspiration, which reduces surface water and dries out soils and vegetation. This condition makes periods with low rainfall drier than they would be in normal conditions, thus resulting in extreme droughts. The extreme drought conditions are more likely to occur in the study area in view of the rising temperatures and the likelihood of low rainfalls and drier months. The resulting effects of the expected, extreme drought conditions are that, residents in the NCA and surrounding areas may have limited access to water for household purposes such as drinking, cooking, cleaning, agriculture,

and livestock keeping, as well as wildlife and tourist activities. Droughts can also raise water prices, force rationing, and even devastate vital water sources like wells during drought years, which necessitates increased water storage during the rainfall period. Previous studies (Estes et al., 2006, Tarver et al., 2019) have reported recurrence of drought conditions, which have led to water shortages in many parts of the NCA. This study indicates the decrease in rainfall with an increase in temperature during JJAS seasons, which anticipate severe droughts conditions during JJAS seasons.

Likewise, the projected increase in rainfall could increase some vector-borne diseases including malaria that would negatively affect the community health of the area (Shukla et al., 2016, Sigdel and Ma, 2016, Githeko et al., 2000, Martin et al., 2008). Outbreaks of diseases such as the Rift Valley fever (RVF), which are common all-over East Africa, are associated with extreme precipitation and floods (Huang et al., 2011, Martin et al., 2008). Already livestock disease outbreaks related to intense droughts have been reported in the study area, killing more than 90% of the calves in the year 2007/2008 (Tarver et al., 2019, Martin et al., 2008). This indicates that the projected temperature rise poses serious threats to the key resources of the NCA and could severely affect the area's tourism business (Tarver et al., 2019). Besides, the Intergovernmental Panel on Climate Change (IPCC) has stipulated those resources such as wildlife, archaeological sites, natural landscapes, and lifestyles/cultures of the local communities surrounding areas such as the NCA are sensitive to climate change impacts (Mkiramweni et al., 2016, IPCC 2007, Martin et al., 2008) further emphasized that this vulnerability to climate change may be high in areas where human-environment interactions exist.

Several studies, e.g., (Serdeczny et al., 2016, Galvin et al., 2004, Guan et al., 2015, Thornton et al., 2011) have argued that, in different parts of Africa, the projected change in climate, warming in temperature, and the expected variability and change in precipitation will pose a significant threat to agriculture and livestock production as well as Africa's hydrological systems. As an important economic sector, agriculture contributes around 25.8% of Tanzania's GDP and comprises up to 40% of the export earnings (Shemsanga et al., 2010, Thornton et al., 2011). Therefore, any significant changes in rainfall and temperature resulting from the changing climate will undoubtedly impact not only the NCA but also the countries earnings. The impacts will go as far as interfering with food security for the growing population (Shemsanga et al., 2010).

Consequently, any proposed adaptation measures must empower local communities in and around the NCA and the relevant sectors to effectively cope with short-term climate changes and reduce the long-term negative impacts of climate change (United Republic of Tanzania 2007, Tumbo et al., 2010, Quenum et al., 2020, Lobell, 2014). These adaptation measures should cut across the various sectors, and most importantly, overlapping sectors like agriculture and tourism. Some adaptation measures that could help may include the following: improving rainwater storage facilities for safe and clean drinking and irrigation water during the dry periods; reducing the anthropogenic impacts on the NCA – tourism and other control over local human activities (Żaba and Gaidzik, 2011b, Kilungu et al., 2017, Orinda and Murray, 2005); growing drought-resistant crops; and changing the planting seasons (Sayasane et al., 2016, Kang et al., 2009, Saba et al., 2013, Smit and Wandel, 2006). Therefore, to cope with the projected changes in rainfall and temperature in the NCA, and better manage the impacts on the fringing communities, these adaptation strategies are crucial.

## 5. Conclusions

In the present study, the CanESM2 global climate model datasets were downscaled and used to project the climate of watersheds surrounding the NCA in Northern Tanzania. During calibration and validation, the model showed high capability in reproducing station rainfall and temperature data. Although the simulated NCEP and CanESM2 data for the daily rainfall showed a weak correlation, the model simulated the monthly and seasonal rainfall, minimum and maximum temperature fairly well. It can be concluded that the model performed better in simulating the temperature data compared to the rainfall data for the daily series and performed well for all parameters for monthly and seasonal simulations. The SDSM output, CORDEX RCMs and LARS-WG downscaled results for rainfall and temperature data were integrated to determine the ensemble mean at a point scale that was applied for climate change analysis by comparing them with historical (1982-2011) data. A comparison between future projections and the historical data showed an increase in rainfall for all seasons except the JJAS season, which shows a decreasing trend for both RCP4.5 and RCP8.5. However, the annual rainfall showed an increase for 2021-2050 period for both RCPs. Likewise, for the maximum and minimum temperatures, the annual increase in temperature would occur in the future for both RCPs, with a higher rise predicted under RCP8.5. Spatially, the highest increase in rainfall would generally occur from central to the southern parts of the study area for all future periods under both RCP4.5 and RCP8.5. For the maximum and minimum temperature, the highest rise would occur over the central and southern parts of the study area for all future periods and RCPs.

The projected increase in rainfall and temperature, both maximum and minimum, over the study area, call for development of adaptation measures and strategic plan for the ecosystem management of the NCA and surrounding areas. The obtained results can be used for performing impact assessment studies which will be useful in addressing the climate change risks and vulnerability in and around the NCA.

## Funding

No funding information to declare.

## Availability of data and materials

Not applicable.

## Code availability

Not applicable.

## Author Contributions

Ideation and conceptualization, MM and MJR; methodology and first draft, MM and IL; analysis and case evaluation, MM and IL; data validation and manuscript logical flow, MM, BKY, SS, DK and MJR; final draft scrutiny and reference management, MM, MJR, AML, SS and SQD; English language structure and grammar check, BKY, AML, SQD, SS and MJR. Moreover, all authors have read and agreed to the published version of the manuscript.

## Conflict of Interest

Authors confirm that no conflict of interest in submitting this article for the publication.

## Acknowledgments

The authors are thankful to the Water Infrastructure and Sustainable Energy Futures (WISE-Futures) Center for their support during this study. We thank the Tanzania Meteorological Authority (TMA) for quality input datasets to facilitate this study. Special appreciation also goes to the former project supervisor, the late Prof. Alfred N. N. Muzuka, who passed on during the course of this work, for the foundations laid for this study.

## References


Adhikari, U., Nejadhashemi, A.P., Woznicki, S.A., 2015. 2018. Climate change and eastern Africa: a review of impact on major crops. Food and Energy Security 4 (2), 110–132. doi:10.1002/fes3.61.

Amirabadizadeh, M., Ghazali, A.H., Huang, Y.F., Wayayok, A., 2016. Downscaling daily precipitation and temperatures over the Langat River Basin in Malaysia: A comparison of two statistical downscaling approaches. International Journal of Water Resources and Environmental Engineering 8 (December), 120–136. doi:10.5897/IJWREE2016.0585.

Bessah, E., Boakye, E.A., Agodzo, S.K., Nyadzi, E., Larbi, I., Awotwi, A., 2021. Increased seasonal rainfall in the twenty-first century over Ghana and its potential implications for agriculture productivity. Environment, Development and Sustainability 1–24.

Bessah, E., Raji, A.O., Taiwo, O.J., Agodzo, S.K., Ololade, O.O., 2019. The impact of varying spatial resolution of climate models on future rainfall simulations in the Pra river basin (Ghana). Journal of Water and Climate Change 11 (4), 1263–1283 https://doi.org/ 10.2166/wcc.2019.258.

Chiew, FHS., Teng, J., Vaze, J., Perraud, J.M., Kirono, D.G.C., Viney, N.R., 2009. Estimating climate change impact on runoff across southeast Australia: Method, results, and implications of the modeling method. Water Resources Research 45 (10), 1–17. doi:10.1029/2008WR007338.

Chen, H., Guo, J., Zhang, Z., Xu, C.Y., 2013. Prediction of temperature and precipitation in Sudan and South Sudan by using LARS-WG in future. Theoretical and Applied Climatology 113 (3), 363–375.

Cooper, P.J.M., Dimes, J., Rao, K.P.C., Shapiro, B., Shiferaw, B., Twomlow, S., 2008. Coping better with current climatic variability in the rain-fed farming systems of sub-Saharan Africa: An essential first step in adapting to future climate change? Agric. Ecosyst. Environ. 126, 24–35. doi:10.1016/j.agee.2008.01.007.

Donat, G.M, Lowry, L.A., Alexander, V.L., O'Gorman, A.P., Maher, N., 2016. More extreme precipitation in the world's dry and wet regions. Nature and Climate change. Vol 6, 508–513. doi:10.1038/nclimate2941.

Estes, R.D., Atwood, J.L., Estes, A.B., 2006. Downward trends in Ngorongoro Crater ungulate populations 1986-2005: Conservation concerns and the need for ecological research. Biological Conservation. 131, 106–120. doi:10.1016/j.biocon.2006.02.009.

Funk, C., Peterson, P., Landsfeld, M., Pedreros, D., Verdin, J., Shukla, S., Husak, G., Rowland, J., Harrison, L., Hoell, A., 2015. The climate hazards infrared precipitation with stations a new environmental record for monitoring extremes. Scientific Data 2 (150066) https://doi.org/10.1038/sdata.2015.66.

Galvin, K.A., Thornton, P.K., Boone, R.B., Sunderland, J., 2004. Climate variability and impacts on East African livestock herders: The Maasai of Ngorongoro Conservation Area. Tanzania. African Journal of Range & Forage Science. 21 (3), 183–189. doi:10.2989/10220110409485850.

Gebrechorkos, S.H., Hülsmann, S., Bernhofer, C., 2019. Statistically downscaled climate dataset for East Africa. Scientific data. 6, 31. doi:10.1038/s41597-019-0038-1, 2019.

Gebrechorkos, S.H., Hülsmann, S., Bernhofer, C., 2018. Evaluation of multiple climate data sources for managing environmental resources in East Africa. Hydrology and Earth System Sciences 22, 4547–4564. doi:10.5194/hess-22-4547-2018.

Githeko, A.K., Lindsay, S.W., Confalonieri, U.E., Patz, J.A., 2000. Climate change and vector-borne diseases: a regional analysis. Bulletin of the World Health Organization 78 (9), 1136–1147.

Gulacha, M.M., Mulungu, D.M.M., 2017. Generation of climate change scenarios for precipitation and temperature at local scales using SDSM in Wami-Ruvu River Basin Tanzania. Physics and Chemistry of the Earth 100, 62–72. doi:10.1016/j.pce.2016.10.003, 2017.

Guan, K., Sultan, B., Biasutti, M., Baron, C., Lobell, D.B., 2015. What aspects of future rainfall changes matter for crop yields in West Africa? Geophysical Research Letters. 42, 8001–8010. doi:10.1002/2015GL063877.

Hashmi, M.Z., Shamseldin, A.Y., Melville, B.W., 2009. Statistical downscaling of precipitation: state-of-the-art and application of bayesian multi-model approach for uncertainty assessment. Hydrol. Earth Syst. Sci. Discuss 5 (5), 6535–6579. doi:10.5194/hessd-6-6535-2009.

Huang, J., Zhang, J., Zhang, Z., Xu, C.Y., Wang, B., Yao, J., 2011. Estimation of future precipitation change in the Yangtze River basin by using statistical downscaling method. Stochastic Environmental Research and Risk Assessment 25 (6), 781–792.

Huang, J., Zhang, J., Zhang, Z., Xu, C.Y., Wang, B., Yao, J., 2011. Estimation of future precipitation change in the Yangtze River basin by using statistical downscaling method. Stochastic Environmental Research and Risk Assessment 25, 781–792. doi:10.1007/s00477-010-0441-9.

IPCC, 2007. Climate change impacts, adaptation and vulnerability: Contribution of working group II to the fourth assessment report of the Intergovernmental Panel on Climate Change Geneva, Switzerland. 2007.

IPCC, 2012. Managing the Risks of Extreme Events and Disasters to Advance Climate Change Adaptation: A Special Report of Working Groups I and II of the Intergovernmental Panel on Climate Change. Cambridge University Press, Cambridge, UK. and New York, NY, p. 2012.

IPCC, 2014, Climate Change 2014: Synthesis Report. Contribution of Working Groups I, II and III to the Fifth Assessment Report of the Intergovernmental Panel on Climate Change [Core Writing Team. In: Pachauri, R.K., Meyer, L.A. (Eds.). IPCC, Geneva, Switzerland, p. 151 eds.].

Kang, Y., Khan, S., Ma, X., 2009. Climate change impacts on crop yield, crop water productivity and food security A review. Progress in Natural Science 19 (12), 1665–1674. doi:10.1016/j.pnsc.2009.08.001.

Kilungu, H., Leemans, R., Munishi, P.K.T., Amelung, B., 2017. Climate Change Threatens Major Tourist Attractions and Tourism in Serengeti National Park, Tanzania. Climate Change Adaptation in Africa. 375–392. doi:10.1007/978-3-319-49520-0_23.

Kim, J., Waliser, D.E., Mattmann, C.A., Goodale, C.E, Hart, A.F, Zimdars, P.A, Daniel, J., 2013. Evaluation of the CORDEX-Africa multi-RCM hindcast: systematic model errors. Clim Dyn 42 (5–6), 1189–1202. doi:10.1007/s00382-013-1751-7.

Larbi, I., Hountondji, F.C.C., Annor, T., Agyare, W.A., Gathenya, J.M., Amuzu, J., 2018. Spatio-temporal trend analysis of rainfall and temperature extremes in the Vea catchment. Ghana. Climate. 6, 1–17. doi:10.3390/cli6040087.

Larbi, I., Nyamekye, C., Hountondji, F.C.C., Okafor, G.C., Odoom, P.E.R., 2021. Climate change impact on climate extremes and adaptation strategies in the Vea catchment, Ghana. In: Leal Filho, W., Ogugu, N., Adelake, L., Ayal, D., da Silva I., I. (Eds.), African Handbook of Climate Change Adaptation. Springer Nature Switzerland AG, Cham, Switzerland, p. 6330, Gewerbestrasse 11. doi:10.1007/978-3-030-42091-8_95-1.

Lawuo, AZ., Mbasa, B., Mnyawi, S., 2014. Persistence of Land Conflicts Between Maasai Community and Ngorongoro Conservation Area Authority (NCCA) in Ngorongoro Conservation Area (NCA). International Journal of Innovation and Scientific Research. ISSN 5, 2351–8014.

Li, X., Babovic, V., 2019. Multi-site multivariate downscaling of global climate model outputs: an integrated framework combining quantile mapping, stochastic weather generator and Empirical Copula approaches. Climate Dynamics 52, 5775–5799. doi:10.1007/s00382-018-4480-0.

Lobell, B.D., 2014. Climate change adaptation in crop production: beware of illusions. Glob Food Sec. 1–5 doi:10.1016/j.gfs.2014.05.002.

López-Moreno, I.J., Vicente-Serrano, M.S., Moran-Tejeda, E., Zabalza, J., Lorenzo-Lacruz, J., García-Ruiz, M.J., 2011. Impact of climate evolution and land use changes on water yield in the Ebro basin. Hydrology and Earth System Science 15, 311–322. doi:10.5194/hess-15-311-2011.

Luhunga, P.M., Kijazi, A.L., Chang'a, L., Kondowe, A., Ng'ongolo, H., Mtongori, H., 2018. Climate change projections for Tanzania Based on high-resolution regional climate models from the Coordinated Regional Climate Downscaling Experiment (CORDEX)-Africa. Frontiers in Environmental Science 6, 1–20. doi:10.3389/fenvs.2018.00122.

Martin, V., Chevalier, V., Ceccato, P.N., Anyamba, A., De Simone, L., Lubroth, J., Domenech, J., 2008. The impact of climate change on the epidemiology and control of Rift Valley fever. Revue Scientifique et Technique, Office International des Epizooties. 27 (2), 413–426.

Masao, C.A., Revocatus, M., Hussein, S., 2015. Will Ngorongoro Conservation Area remain a world heritage site amidst increasing human footprint? International Journal of Biodiversity and Conservation 7, 394–407. doi:10.5897/ijbc2015.0837.

Mkiramweni, N.P., DeLacy, T., Jiang, M., Chiwanga, F.E., 2016. Climate change risks on protected areas ecotourism: shocks and stressors perspectives in Ngorongoro Conservation Area. Tanzania. Journal of Ecotourism. 15, 139–157. doi:10.1080/14724049.2016.1153645.

Moriasi, D.N., Gitau, M.W., Pai, N., Daggupati, P., 2015. Hydrologic and water quality models: Performance measures and evaluation criteria. Transactions of the ASABE 58 (6), 1763–1785. doi:10.13031/trans.58.10715.

Molua, E.L., 2009. An empirical assessment of the impact of climate change on smallholder agriculture in Cameroon. Global and Planetary Change 67 (3–4), 205–208. doi:10.1016/j.gloplacha.2009.02.006.

Mtongori, H.I., Stordal, F., Benestad, R.E., 2016. Evaluation of empirical statistical downscaling models' skill in predicting Tanzanian rainfall and their application in providing future downscaled scenarios. Journal of Climate 29 (9), 3231–3252. doi:10.1175/JCLI-D-15-0061.1.

Nkiaka, E., Nawaz, N.R., Lovett, J.C., 2017. Evaluating global reanalysis precipitation datasets with rain gauge measurements in the Sudano-Sahel region: case study of the Logone catchment. Lake Chad Basin. Meteorological Applications. 24, 9–18. doi:10.1002/met.1600.

Obuobie, E., Kankam-Yeboah, K., Amisigo, B., Opoku-Ankomah, Y., Ofori, D., 2012. Assessment of water stress in river basins in Ghana. Journal of Water and Climate Change 03 (4), 276–286. doi:10.2166/wcc.2012.030.

Orinda, V.A., Murray, L.A., 2005. Adapting to climate change in East Africa: a strategic approach. Gatekeeper Series 117, 2005 International Institute for Environment and Development..

Osman, Y.Z., Abdellatif, M.E., 2016. Improving accuracy of downscaling rainfall by combining predictions of different statistical downscale models. Water Science 30 (2), 61–75. doi:10.1016/j.wsj.2016.10.002.

Quenum, G.M.L.D., Klutse, N.A.B., Alamou, E.A., Lawin, P.G., 2020. Precipitation Variability in West Africa in the Context of Global Warming and Adaptation Recommendations. African Handbook of Climate Change Adaptation 1–22. doi:10.1007/978-3-030-42091-8_85-1.

Saba, A., Gerrard, M.B., Lobell, D.B., 2013. Getting ahead of the curve: supporting adaptation to long-term climate change and short-term climate variability alike. Carbon and Climate Law Review 3–23.

Saraf, V.R., Regulwar, D.G., 2016. Assessment of Climate Change for Precipitation and Temperature Using Statistical Downscaling Methods in Upper Godavari River Basin. India. Journal of Water Resource and Protection. 08, 31–45. doi:10.4236/jwarp.2016.81004.

Sayasane, R., Kawasaki, A., Shrestha, S., Takamatsu, M., 2016. Assessment of potential impacts of climate and land use changes on streamflow: A case study of the Nam Xong watershed in Lao P.D.R. Journal of Water and Climate Change. 7, 184–197. doi:10.2166/wcc.2015.050.

Semenov, M.A., Barrow, E.M., 2002. A Stochastic Weather Generator for Use in Climate Impact Studies. User Manual. Hertfordshire, UK, pp. 0–27 (2002).

Serdeczny, O., Adams, S., Baarsch, F., Coumou, D., Robinson, A., Hare, B., Schaeffer, M., Perrette, M., Reinhardt, J., 2016. Climate change impacts in Sub-Saharan Africa: from physical changes to their social repercussions. Reg. Environ. Change. 1–16. doi:10.1007/s10113-015-0910-2.

Shemsanga, C., Omambia, A.N., Gu, Y., 2010. The Cost of Climate Change in Tanzania: Impacts and Adaptations. Journal of American Science 6 (3), 182–196. doi:10.4236/ajcc.2014.32011.

Shukla, R., Khare, D., Deo, R., 2016. Statistical downscaling of climate change scenarios of rainfall and temperature over Indira Sagar canal command area in Madhya Pradesh, India. In: Proceedings - 2015 IEEE 14th International Conference on Machine Learning and Applications, ICMLA., pp. 313–317. doi:10.1109/ICMLA.2015.75.

Sigdel, M., Ma, Y., 2016. Evaluation of future precipitation scenario using statistical downscaling model over humid, subhumid, and arid region of Nepal—a case study. Theoretical and Applied Climatology 123, 453–460. doi:10.1007/s00704-014-1365-y.

Smit, B., Wandel, J., 2006. Adaptation, adaptive capacity and vulnerability. Global Environmental Change 16 (3), 282–292. doi:10.1016/j.gloenvcha.2006.03.008.

Tarver, R., Cohen, K., Klyve, D., Liseki, S., 2019. Sustainable safari practices: Proximity to wildlife, educational intervention, and the quality of experience. Journal of Outdoor Recreation and Tourism 25, 76–83. doi:10.1016/j.jort.2019.01.001.

Thornton, P.K., Jones, P.G., Ericksen, P.J., Challinor, A.J., 2011. Agriculture and food systems in sub-Saharan Africa in a 4 C+ world. Philosophical Transactions of the Royal Society A: Mathematical. Physical and Engineering Sciences 369, 117–136. doi:10.1098/rsta.2010.0246, (1934).

Tumbo, S., Mpeta, E., Tadross, M., Kahimba, F., Mbillinyi, B., Mahoo, H., 2010. Application of self-organizing maps technique in downscaling GCMs climate change projections for Same, Tanzania. Physics and Chemistry of the Earth, Parts A/B/C, 35 (13-14), 608–617. doi:10.1016/j.pce.2010.07.023.

United Republic of Tanzania, 2007. National adaptation programme of action (NAPA). Vice president's office, division of environment. Government printers, Dar es Salaam, p. 2007.

United Republic of Tanzania, 2008. State of the environment report. Vice President'soffice, Division of Environment, Dar es Salaam, p. 2008.

Wambura, F., S.Tumbo, H.Ngongolo, Mlonganile, P., Sangalugembe, C., 2014b. Tanzania CMIP5 climate change projections. In: Proceedings of the International Conference on Reducing Climate Change Challenges through Forestry and Other Land Use Practices 2014b.

Westberg, D.J., Stackhouse Jr, P.W., Hoell, J.M., Chandler, W.S., 2013. An analysis of NASA's MERRA meteorological data to supplement observational data for calculation of climatic design conditions. ASHRAE Transactions 119 (210).

Wilby, R.L., Dawson, C.W., Barrow, E.M., 2002. SDSM - A decision support tool for the assessment of regional climate change impacts. Environmental Modelling and Software. 17, 145–157. doi:10.1016/s1364-8152(01)00060-3.

Wilby, R.L., Dawson, C.W., 2013. The Statistical DownScaling Model: insights from one decade of application. International Journal of Climatology 33 (7), 1707–1719 https://doi.org/10.1002/joc.3544.

Żaba, J., Gaidzik, K., 2011. The Ngorongoro Crater as the biggest geotouristic attraction of the Gregory Rift (Northern Tanzania, Africa) – geographical setting. Geotourism/Geoturystyka. 3, 24–25. doi:10.7494/geotour.2011.24-25.3.

Żaba, J., Gaidzik, K., 2011. The Ngorongoro Crater as the biggest geotouristic attraction of the Gregory Rift (Northern Tanzania, Africa) geotouristic valorization. touristic development and hazard. Geotourism/Geoturystyka 24–25 47. doi:10.7494/geotour.2011.24-25.47.